SEMARAK ILMU PUBLISHING

Semarak International Journal of Fundamental and Applied Mathematics

Journal homepage:
https://semarakilmu.my/index.php/sijfam
ISSN: 3030-5527

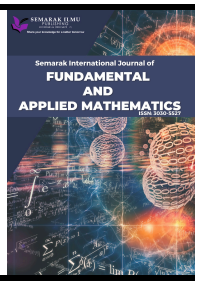

Type-2 Fuzzy Number-Based Intuitionistic Fuzzy Interpolation Bezier Curve Modeling

Rozaimi Zakaria[1,*], Wilvaldo Dousip[2], Rodeano Roslee[3], Suzelawati Zenian[4], Mohammad Izat Emir Zulkifly[5]

[1] Mathematics Visualization (MathViz) Research Group, Faculty of Science and Technology, Universiti Malaysia Sabah, Jalan UMS, 88400 Kota Kinabalu, Sabah, Malaysia
[2] Faculty of Science and Technology, Universiti Malaysia Sabah, Jalan UMS, 88400 Kota Kinabalu, Sabah, Malaysia
[3] Department of Mathematics, Faculty of Sciences, University of Technology Malaysia (UTM), Johor Bahru, Malaysia

ARTICLE INFO

Article history:
Received 8 June 2025
Received in revised form 29 July 2025
Accepted 10 August 2025
Available online 30 September 2025

Keywords:
Type-2 fuzzy number; intuitionistic fuzzy number; Bezier Curve; interpolation; alpha value; earthquake magnitude data

ABSTRACT

The challenge is to accurately evaluate uncertainty in imprecise data in complicated systems, particularly when the data is subjective or based on measurements that are very inaccurate. This paper shows a new method of accomplishing things by using a Bézier curve interpolation framework with Type-2 fuzzy numbers (T2FNs) and intuitionistic fuzzy sets. The T2FN based Intuitionistic fuzzy interpolation Bézier Curve that is being spoken about here exhibits uncertainty in two ways which are via secondary membership functions and hesitation degrees. This is great for data that is highly unclear. The way the construction is done mixes the flexibility of Bézier curve geometry with the more expressive T2FN and intuitionistic fuzzy notions. We test the model with both fake and genuine data, including earthquake magnitude data that fluctuates a lot. The experiment's results suggest that the T2FN-IFIBC is superior at handling data uncertainty because it makes curve fitting more stable and adaptable. When faced with ambiguous data, this technique empowers the maximization of the potential of geophysical modeling, risk analysis, and data analytics, enabling the achievement of extraordinary results.

1. Introduction

The main goal of data modeling is to show, analyze, and get insights from environmental data. Data modeling is important because it can create abstract models of complicated systems that may help us understand and control the underlying environmental dynamics. Zhang et al. say that fuzzy set theory is important for dealing with the uncertainties that come with external elements like economic circumstances and vendor rates. This lets you handle these uncertainties in an organized way when making decisions [1]. Also, fuzzy measures and integrals have been used to improve risk coordination in the supply chain. This shows how data modeling efforts directed at environmental

* *Corresponding author.*
E-mail address: rozaimi@ums.edu.my

https://doi.org/10.37934/sijfam.8.1.128

data may be used in real life [1]. This modeling does more than just show data; it also lets you manipulate and understand data complexity in a variety of situations, such as supply chain management and ecological evaluations.

Adding uncertainty to data modeling, on the other hand, may make things harder. There are a variety of factors that might make things hard to understand, such wrong measurements, changes in the environment, or missing data. The existence of these ambiguous elements complicates the determination of appropriate actions and the assessment of potential risks. Jifrin *et al*., [2] indicate that fuzzy set theory, along with other methodologies, may facilitate the analysis of data that is unclear or erroneous. This may make it tricky to model, particularly when it comes to interpolating coastline data [2]. If the evidence is highly obscure, the remaining probability may not match what really occurred. If this process is not executed properly, it may lead to inaccurate conclusions. Fuzzy set theory can assist in addressing uncertainties. However, its efficacy may diminish as the complexity of the situation increases.

As uncertainties escalate, particularly within complex systems or datasets, traditional fuzzy set theory may prove inadequate in fully capturing the breadth of the uncertainties encountered. Type-2 fuzzy sets (T2FSs) present an enhanced framework that significantly improves the representation of uncertainty by allowing variability in the membership functions themselves. Type-2 fuzzy logic systems (T2FLSs) have garnered attention due to their capability to effectively model uncertainties arising from various sources, such as measurement noise or fluctuating environmental conditions [3, 4]. Research has shown that T2FSs excel in handling scenarios characterized by higher degrees of vagueness and ambiguity, outperforming conventional fuzzy approaches that rely solely on deterministic membership values [5,6]. These advanced fuzzy systems provide additional degrees of freedom through the concept of a "Footprint of Uncertainty" (FOU), which robustly characterizes uncertainty by encompassing a broader spectrum of possible membership values [7,8]. Consequently, T2FSs create a more realistic and nuanced representation of complex environmental data, addressing the intrinsic challenges that simpler fuzzy models often overlook [9]. This capability positions type-2 fuzzy logic not only as a theoretical advancement but also as a crucial tool in practical fields requiring precise modeling of uncertainty, such as environmental management and control systems [10].

In the face of challenges, it is essential to cultivate innovative approaches to address the issues that arise, particularly in the context of T2FS applications that utilize alpha values. Intuitionistic fuzzy sets (IFSs) incorporate the elements of membership, non-membership, and hesitation, offering a unique methodology for representing uncertainty. This comprehensive framework surpasses conventional fuzzy methods in representing ambiguity. IFSs offer significant benefits in situations marked by a multitude of unknown variables and defined eligibility requirements for involvement [11,12]. Atanassov introduced the concept of intuitionistic fuzzy set theory in the 1980s. It not only comprehends how to navigate the complexities of uncertainty, but it also facilitates the handling of ambiguous data. This suggests that decision-making frameworks could be utilized in further contexts [11,13]. Research conducted by Pomare *et al*., [13] and Wang *et al*., [14] demonstrates that intuitionistic fuzzy sets are beneficial in the healthcare sector, aiding individuals in making more informed decisions. In situations characterized by significant uncertainty, these models demonstrate enhanced performance. This approach enhances fuzzy set theory by integrating innovative perspectives for analyzing various datasets [15,16]. This illustrates the superior capability of IFSs in managing uncertainty in both research and practical scenarios compared to traditional methods. This illustrates their importance in the realm of fuzzy logic applications, which is currently evolving [16].

Researchers can enhance the representation of real-world events in environmental data modeling by employing intuitionistic fuzzy sets, particularly through geometric representations such

as Bézier curves. Zakaria et al. demonstrate that integrating intuitionistic fuzzy sets with rational Bézier surface functions provides a compelling visualization of complex environmental information while highlighting the related uncertainties [17]. This geometric approach enhances the comprehension of intricate uncertainties and fortifies decision-making frameworks that address the inherent complexities of environmental data [9]. This strategy enhances the models' expressiveness by addressing inherent fuzziness and ensuring accurate interpretation of the datasets [9]. Intuitionistic fuzzy sets facilitate the integration of various forms of uncertainty, including membership, non-membership, and hesitation. This enhances the accuracy of environmental evaluations and predictions . Furthermore, frameworks that employ intuitionistic fuzzy set are especially adept at clarifying uncertainties present in various environmental contexts. This enhances the reliability of data analyses and the processes associated with decision-making [18]. The integration of intuitionistic fuzzy sets with geometric models provides valuable instruments that assist in addressing the complex nature of environmental phenomena. This facilitates the development of improved strategies for environmental management.

To address uncertainty in environmental data, it is essential to implement a thorough strategy that incorporates fuzzy set theory, T2FSs, and intuitionistic fuzzy sets. This method offers a more accurate depiction of intricate data landscapes. The integration of these methods improves the modeling process by accommodating various membership functions and providing the flexibility needed to address uncertain conditions. This, in turn, enhances the reliability and effectiveness of assessments across diverse fields including environmental science and financial forecasting [19]. Recent advancements underscore the promise of employing fuzzy logic in real-time environmental monitoring, particularly when combined with Internet of Things (IoT) technologies, to enhance data collection and adaptive control systems for addressing uncertainties in environmental data [10,20]. Furthermore, fuzzy logic systems have demonstrated significant efficacy in the creation of predictive models, especially in the realm of demand forecasting, where precise data interpretation is essential in the face of uncertainty [21]. Through the systematic integration of these methodologies, one can develop models that exhibit resilience and adaptability, thereby effectively tackling the complexities inherent in real-world datasets and the challenges presented by uncertain information [22,23].

This paper is structured in the following manner: Section 2 outlines the methodology employed in the development of the proposed model. Section 3 presents the outcomes derived from Section 2, including the mathematical equation that illustrates the application of the model to a case study. This is followed by a discussion of the results in Section 4. In conclusion, Section 5 provides a summary of the findings and offers recommendations for future research.

2. Methodology

In this methodology, the approach employs T2FNs, intuitionistic fuzzy numbers, and interpolation Bézier curves in an innovative way to represent earthquake magnitude data. The application of T2FN improves the handling of uncertainty by offering a more profound understanding of the imprecision inherent in the data. The model incorporates intuitionistic fuzzy numbers, adeptly capturing both membership and non-membership degrees, thereby providing a comprehensive insight into uncertainty. Bezier curves are employed to illustrate trends and relationships present in the data through curve visualization. This provides a comprehensive and precise assessment of earthquake intensity across historical timelines. This approach enhances the accuracy and reliability of earthquake size predictions, establishing it as a crucial instrument for seismological assessment.

2.1 Data Collection

The magnitude of earthquakes was sourced from the Malaysian Meteorological Department, commonly referred to as MetMalaysia. The dataset includes historical records of earthquakes occurring in Malaysia, with a particular focus on Ranau in Sabah. Between January 2017 and December 2017, a total of 55 seismic events were documented in Ranau, showing variations in magnitude and geographical distribution.

2.2 Type-2 Fuzzy Number in Defining Uncertainty Complex Data

T2FNs are very important for finding and dealing with data that is hard to understand. They help us grasp better things that happen in the actual world that are naturally unclear or obscure. The basic ideas behind type-1 fuzzy sets are used to create T2FSs. In a three-dimensional space, fuzzy sets show membership grades. Zakaria *et al*., [24] say that this technique works well to clear up any confusion about these grades. This trait makes T2FSs better at handling more uncertainty than regular fuzzy sets. This is useful in fields including risk analysis, environmental modeling, and multi-criteria decision-making [25,26].

The integration of T2FNs facilitates the representation of multiple types of uncertainty, such as linguistic uncertainty, measurement errors, and the intrinsic variability present in observed data [9]. The use of T2FSs in the construction of Bézier curves allows for the representation of uncertainty in control points, improving the visualization of complex datasets where conventional methods might struggle, as Zakaria and colleagues' research [27]. This holds significant value in environmental contexts, including the modeling of shoreline data or geological hazards, where uncertainties are common and can greatly influence decision-making processes [9,27].

2.3 Intuitionistic Fuzzy Number

The utilization of intuitionistic fuzzy numbers in data modeling, especially for curve representation, greatly enhances the handling of uncertainties faced in real-world situations. Atanassov introduced intuitionistic fuzzy sets, which provide benefits over traditional fuzzy sets by integrating a membership function, a non-membership function, and a degree of hesitation. This method facilitates a more thorough representation of data, thereby aiding in the resolution of uncertainties that may occur in various contexts. The studies carried out by Davvaz et al. [28] and Ejegwa and Adamu [29] hold significant relevance. This thorough approach is particularly advantageous for modeling intricate datasets, as it offers various options for representing uncertain data. Zulkifly and Wahab [30] illustrated that intuitionistic fuzzy Bézier curves, developed through the integration of Bernstein polynomials with intuitionistic fuzzy control points, proficiently capture uncertainty in data. This enables informed decision-making in multiple areas, including engineering and environmental management [30,31].

The utilization of intuitionistic fuzzy numbers in conjunction with geometric models enables the creation of an advanced and dynamic representation of datasets, incorporating both membership and non-membership degrees. This produces better results than traditional models. Research shows that intuitionistic fuzzy models are effective in tackling challenges related to uncertain data in areas like pattern recognition and image segmentation, where hesitation and ambiguity are significant factors [32,33]. Analysts can employ these models to generate visualizations that clearly illustrate the uncertainty present in the data, while also supporting strong predictions and flexible decision-making. This improves the reliability of data modeling in fields like artificial intelligence and

environmental science. The integration of curves with intuitionistic fuzzy sets in data modeling signifies a notable progression in tackling ambiguity challenges, positioning it as an essential tool in modern analysis.

2.4 Piecewise Interpolation Bezier Curve

Piecewise Bézier curve interpolation is a widely used method in computer graphics for modeling data sets, offering an effective way to approximate smooth curves that closely match specified points. Every segment of the Bézier curve is characterized by a distinct set of control points, enabling precise adjustments to the curve's form. This segmentation ensures continuity between segments, resulting in smooth transitions that accurately represent complex shapes while circumventing the computational challenges associated with higher-degree polynomial functions [34]. The implementation of this interpolation is significant in fields like computer-aided geometric design (CAGD), animation, and graphical rendering, where generating visually accurate data representations is crucial [35]. Furthermore, the adaptability of piecewise Bézier curves enables precise modeling of real-world phenomena, making them crucial in applications that require careful detail and smooth representational transitions [34].

In the context of modeling earthquake magnitude data, piecewise Bézier curve interpolation offers a strong framework for analyzing and illustrating the temporal variations in seismic activity. Considering the inherent uncertainties and fluctuations associated with earthquake magnitudes, the application of Bézier curves enables researchers to create models that accurately represent the temporal variations in seismic magnitudes while addressing data discrepancies [36]. This approach provides improved visualization features, assisting researchers in recognizing patterns in seismic activities and possibly predicting future events based on past data. For example, piecewise interpolation adeptly manages significant fluctuations in earthquake magnitudes, facilitating a more precise depiction of seismic activity trends over time and aiding in the formulation of disaster preparedness models. By effectively illustrating the temporal dynamics of seismic measurements, piecewise Bézier curves significantly contribute to our understanding of earthquake phenomena and the enhancement of societal resilience to such natural disasters [37].

3. Result

The implementation of the proposed Type-2 fuzzy interpolation Bézier curve (T2FIBC) model resulted in notable enhancements in the modeling of uncertainty within earthquake magnitude data. The integration of T2FNs with Bézier curve interpolation has resulted in a model that effectively captures the inherent imprecision and ambiguity present in seismic datasets, especially across different magnitude scales. In this section, the mathematical formulation will be established to develop the T2FIBC model, which will subsequently be utilized to model the shoreline data. To enhance comprehension, each definition will be illustrated visually.

Definition 3.1

A T2FN is broadly defined as a T2FS that has a numerical domain. An interval of T2FS is defined using the following four constraints, where $\tilde{\tilde{A}}_{\alpha} = \left\{\left[a^{\alpha}, b^{\alpha}\right], \left[c^{\alpha}, d^{\alpha}\right]\right\}$, $\forall \alpha \in [0,1]$, $\forall a^{\alpha}, b^{\alpha}, c^{\alpha}, d^{\alpha} \in \sim$ (Figure 1):

1. $a^{\alpha} \le b^{\alpha} \le c^{\alpha} \le d^{\alpha}$

2. $[a^{\alpha}, d^{\alpha}]$ and $[b^{\alpha}, c^{\alpha}]$ generate a function that is convex and $[a^{\alpha}, d^{\alpha}]$ generate a normal function.
3. $\forall \alpha_1, \alpha_2 \in [0,1]: (\alpha_2 > \alpha_1) \Rightarrow \left(\left[a^{\alpha_1}, c^{\alpha_1}\right] \supset \left[a^{\alpha_2}, c^{\alpha_2}\right], \left[b^{\alpha_1}, d^{\alpha_1}\right] \supset \left[b^{\alpha_2}, d^{\alpha_2}\right]\right)$, for $c^{\alpha_2} \geq b^{\alpha_2}$.
4. If the maximum of the membership function generated by $[b^{\alpha}, c^{\alpha}]$ is the level α_m, that is $[b^{\alpha_m}, c^{\alpha_m}]$, then $\left[b^{\alpha_m}, c^{\alpha_m}\right] \subset \left[a^{\alpha=1}, d^{\alpha=1}\right]$[27, 38] .

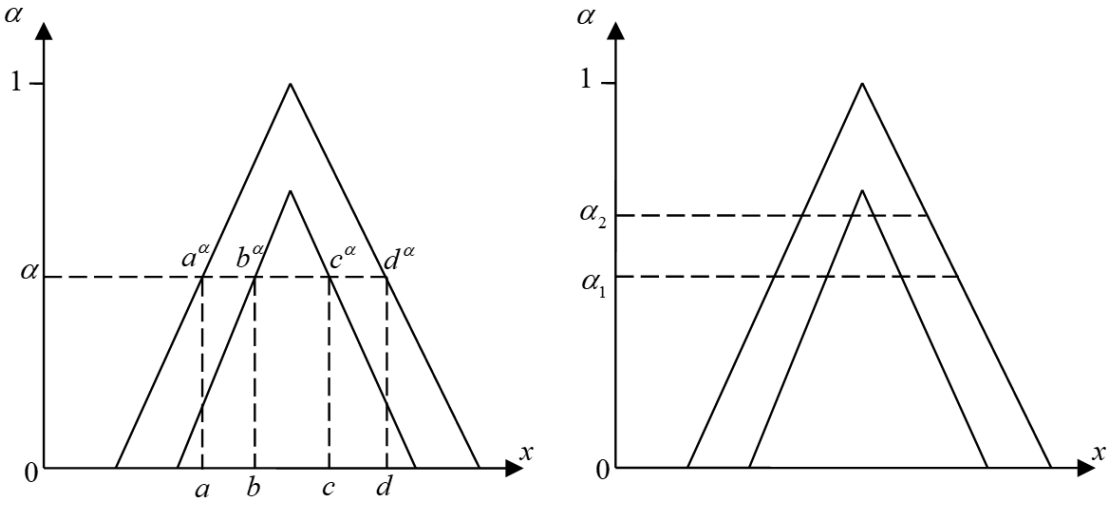

Fig. 1. Definition of an interval T2FN

Figure 1 presents an interval T2FN as defined in Definition 3.1. The outer membership function $\left[a^{\alpha}, d^{\alpha}\right]$ and the inner membership function $\left[b^{\alpha}, c^{\alpha}\right]$ adhere to the ordering $\left[a^{\alpha}, b^{\alpha}\right]$ (Item 1). The outer function exhibits convexity and normality, whereas the inner function establishes the FOU in conjunction with the outer function (Item 2). Horizontal dashed lines at two alpha-levels $(\alpha_1$ and α_2, with $\alpha_2 > \alpha_1)$ illustrate the nesting property, where the α-cut intervals diminish as α increases and are encompassed within the intervals at lower α-values (Item 3). At the maximum membership level $\alpha_m = 1$, the core interval $\left[b^{\alpha_m}, c^{\alpha_m},\right]$ is entirely contained within the corresponding outer boundary $\left[a^{\alpha_m - 1}, d^{\alpha_m - 1},\right]$ item (Item 4), clearly illustrating the bounded uncertainty structure of the T2FN.

Definition 3.2

Let $E = \{x | x \text{ type-2 fuzzy point}\}$ and $\ddot{\tilde{E}} = \left\{E_i \middle| E_i \text{ data point of earthquake magnitude}\right\}$ are type-2 fuzzy earthquake magnitude data (T2FEMD) with $E_i \in E \subset X$, where X is a universal set and $\mu_E(E_i): E \to [0,1]$ is the membership function defined as $\mu_E(E_i) = 1$ and formulated as $\ddot{\tilde{E}} = \left\{\left(E_i, \mu_E(E_i)\right) \middle| E_i \in \tilde{}, i = 0,1,2,...,n\right\}$. Therefore,

$$\mu_E(E_i) = \begin{cases} 0 & if\ E_i \notin X \\ c \in (0,1) & if\ E_i \ddot{\in} X \\ 1 & if\ E_i \in X \end{cases}$$

(1)

with $\mu_E(E_i)=\left\langle \mu_E\left(E_i^{\leftarrow}\right),\mu_E(E_i),\mu_E\left(E_i^{\rightarrow}\right)\right\rangle$ which $\mu_E\left(E_i^{\leftarrow}\right)$ and $\mu_E\left(E_i^{\rightarrow}\right)$ are left and right footprint of membership values with $\mu_E\left(E_i^{\leftarrow}\right)=\left\langle \mu_E\left(aE_i^{\leftarrow}\right),\mu_E\left(bE_i^{\leftarrow}\right)\right\rangle$ where, $\mu_E\left(aE_i^{\leftarrow}\right)$ and $\mu_E\left(bE_i^{\leftarrow}\right)$ are left-left, right-left membership grade values and $\mu_E\left(E_i^{\rightarrow}\right)=\left\langle \mu_E\left(cE_i^{\rightarrow}\right),\mu_E\left(dE_i^{\rightarrow}\right)\right\rangle$ where, $\mu_E\left(cE_i^{\rightarrow}\right)$and $\mu_E\left(dE_i^{\rightarrow}\right)$ are right-right, left-right membership grade values which can be written as $\overleftrightarrow{E}=\left\{\overleftrightarrow{E}_i : i=0,1,2,...,n\right\}$

(2) for every *i*, $\overleftrightarrow{E}_i=\left\langle[a_i,b_i]\right\rangle$ with $a_i=\left\langle\left[aa_i,bb_i\right]\right\rangle$ where aa_i and bb_i are left-left and right-left T2FEMD and $b_i=\left\langle\left[cc_i,dd_i\right]\right\rangle$ where cc_i and dd_i are left-right and right-right T2FEMD respectively. This can be illustrated as in Figure 2.

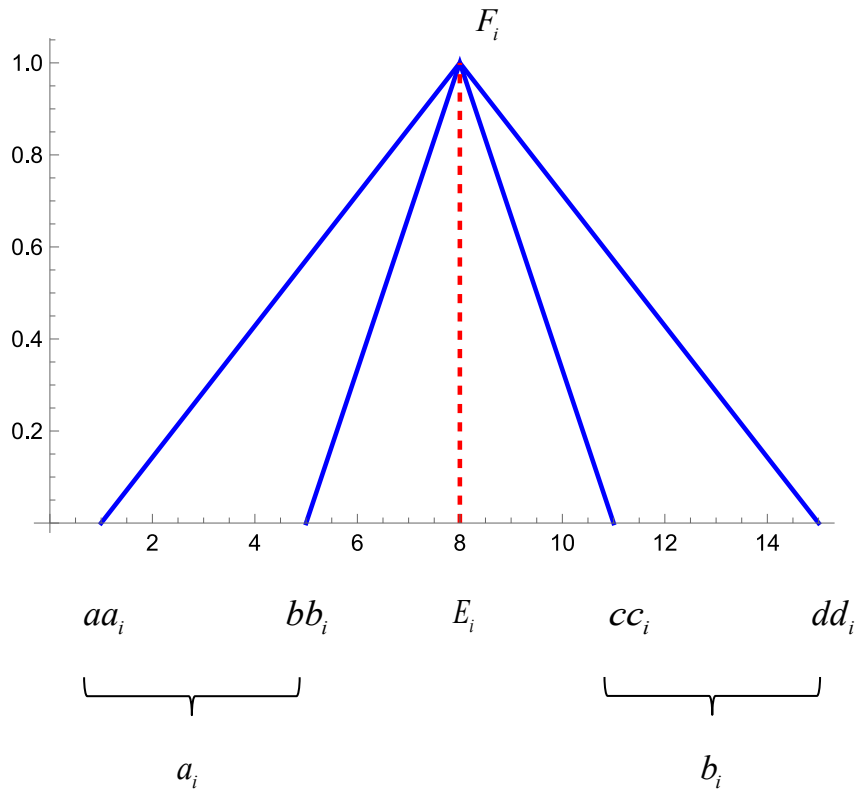

Fig. 2. T2FEMD around 8

Figure 2 presents a T2FEMD point centered around $E_i=8$ as outlined in Definition 3.2. In this context, aa_i, bb_i, cc_i and dd_i denote the boundaries for the left-left, right-left, left-right, and right-right membership grades, respectively. The blue outer triangle represents the FOU defined by the intervals $a_i=\left[aa_i,bb_i\right]$ on the left side of E_i and $b_i=\left[cc_i,dd_i\right]$on the right side, effectively capturing uncertainty in both directions from the central data point. The inner blue triangle denotes the inner membership function, whereas the vertical red dashed line indicates the crisp magnitude value E_i, which corresponds to its peak membership value $F_i=1$. This structure effectively illustrates how

T2FEMD models uncertainty in earthquake magnitude measurements by delineating both the primary magnitude and the range of uncertainty on either side.

Seismologists employ a range of scales to evaluate the magnitude of an earthquake. The four types include Local Magnitude (ML) [39], Body-Wave Magnitude (mb) [40], Surface-Wave Magnitude (Ms) [41], and Moment Magnitude (Mw). Each of these scales is based on different concepts, each having its own strengths and weaknesses. The inherent volatility poses considerable challenges in precisely documenting magnitudes. For example, a single earthquake can display several magnitude readings, fluctuating by ±0.2 to ±1.0 units.

Comprehending the differences between various techniques for quantifying earthquake magnitude, including Local Magnitude (ML), Surface-Wave Magnitude (Ms), and Body-Wave Magnitude (Mb), is essential for the precise evaluation of seismic data. Kadirioğlu and Kartal [42] suggest that machine learning may not exhibit the same level of effectiveness in identifying significant earthquakes when compared to other magnitude scales, especially for magnitudes of 6.0 or higher. On the other hand, Surface-Wave Magnitude may not accurately reflect deep-focus earthquakes, while Body-Wave Magnitude can be affected by crustal characteristics and frequency filtering, which complicates the accuracy of magnitude reporting [43]. Discrepancies of this nature can present considerable challenges in the development of historical earthquake catalogs or in the comparison of events across different tectonic contexts. Researchers frequently utilize conversion equations or probabilistic models to tackle these inconsistencies. However, these traditional approaches may not completely encompass the inherent uncertainty linked to seismic measurements.

T2FNs effectively address this ambiguity. Researchers can utilize T2FNs to demonstrate the spectrum of potential magnitude values along with the associated uncertainty. For example, when an earthquake is documented with ML = 6.5 ± 0.5 and Ms = 6.8 ± 0.3, then a T2FN may represent this data as a fuzzy envelope. This envelope exhibits varying levels of confidence, thereby reducing the likelihood of errors in seismic modeling [44]. This example illustrates the utility of alpha-cuts in deriving intervals from fuzzy sets that correspond to specific confidence levels. This analyzes the intricate fuzzy envelope and deconstructs it into more manageable components for improved handling. This comprehensive analysis of alpha-level intervals enhances our understanding of the propagation of uncertainty in seismic observations. This enables the assessment of earthquake likelihood, especially when combined with methods such as Bézier curve interpolation [45]. Utilizing T2FNs to simulate earthquake magnitudes enhances our understanding of the associated uncertainties significantly. This enables us to thoroughly understand the facts and prepare for various scenarios [46].

Definition 3.3

Let $\ddot{\tilde{E}}_i$ be the set of T2FEMDs with $\ddot{\tilde{E}}_i \in \ddot{\tilde{E}}$ where $i = 0,1,...,n-1$. Then $\ddot{\tilde{E}}_{i_\alpha}$ is the alpha-cut operation of T2FEMDs with $i = 0,1,2,...,n$ which is given as follows.

$$\begin{aligned}
\ddot{\tilde{E}}_{i_\alpha} &= \left\langle a_{i_\alpha}, E_i, b_{i_\alpha} \right\rangle \\
&= \left\langle \left[aa_{i_\alpha}, bb_{i_\alpha} \right], E_i, \left[cc_{i_\alpha}, dd_{i_\alpha} \right] \right\rangle \\
&= \left\langle \left(E_i - \left[aa_{i_\alpha}, bb_{i_\alpha} \right] \right)\alpha + \left[aa_{i_\alpha}, bb_{i_\alpha} \right], E_i, -\left(\left[cc_{i_\alpha}, dd_{i_\alpha} \right] - E_i \right)\alpha + \left[cc_{i_\alpha}, dd_{i_\alpha} \right] \right\rangle
\end{aligned} \tag{3}$$

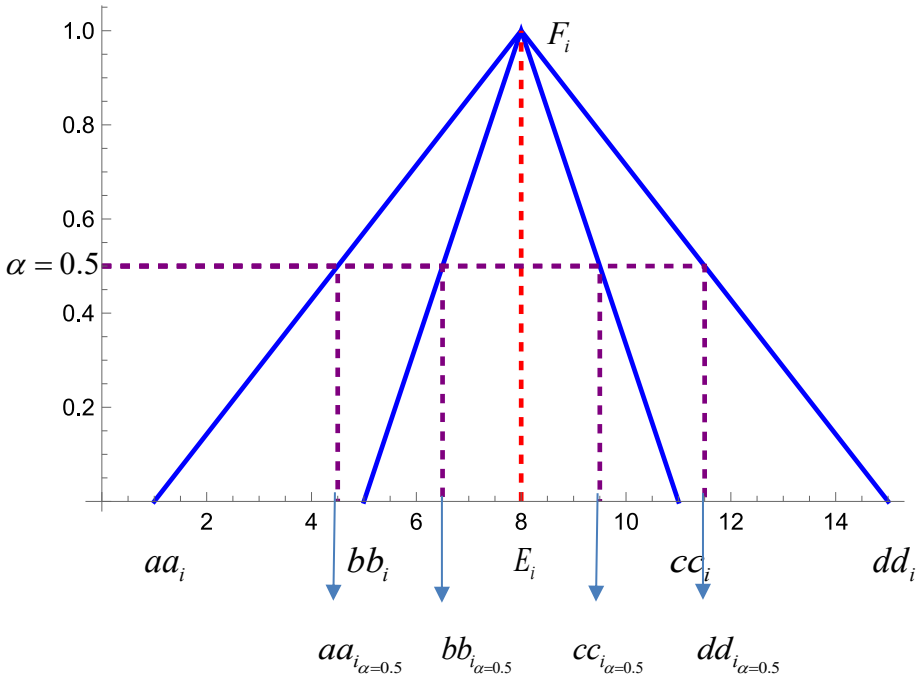

Fig. 3. The alpha-cut operation towards T2FEMD

Figure 3 demonstrates the alpha-cut operation of a T2FEMD as outlined in Definition 3.3. The original T2FEMD is depicted by the outer blue triangle, which encompasses the left and right boundaries (aa_i, bb_i) and (cc_i, dd_i), surrounding the central crisp value E_i. The alpha-cut at $\alpha = 0.5$ is represented by the horizontal dashed purple line, which intersects the membership functions to yield the reduced interval boundaries $aa_{i,\alpha=0.5}$, $bb_{i,\alpha=0.5}$ on the left and $cc_{i,\alpha=0.5}$, $dd_{i,\alpha=0.5}$ on the right. The new points are established through linear interpolation between E_i and the original support endpoints, guided by the alpha value. The vertical dashed purple lines denote the positions of the α-cut boundaries, whereas the red dashed line signifies the location of E_i, characterized by peak membership $F_i = 1$. This operation successfully reduces the FOU to the interval aligned with the specified alpha-level, offering a cross-section of the T2FEMD at a selected degree of membership.

The alpha-cut of a triangular T2FN serves as a method for representing uncertainty by defining specific intervals derived from fuzzy sets according to a specified confidence level (alpha). In this context, T2FNs can demonstrate the potential range of values for a specific phenomenon, such as earthquake magnitudes, along with the associated level of uncertainty pertaining to that range. The centroid, or center of mass, of the triangular fuzzy area is essential for determining the alpha value, providing a structured method for analyzing fuzzy data. The alpha-cut functions as a mechanism to clarify the intricacies of T2FNs by defining particular intervals that align with different confidence levels, thereby enhancing analysis and decision-making in uncertain contexts.

Following the establishment of the alpha-cut, researchers are able to systematically assess the impact of uncertainty on the measurements under evaluation. This methodology assists researchers in identifying specific time frames that exhibit a variety of potential values within the T2FN. This improves the understanding of how uncertainty propagates in seismic evaluations. The alpha-cut plays a crucial role in enhancing the clarity and usability of T2FNs in practical applications, where precise information is vital for assessing risks and making informed predictions regarding events such as earthquakes [46, 47]. The application of alpha-cuts with T2FNs facilitates the development of models that enrich our comprehension of complex data characteristics, thereby improving prediction

accuracy and aiding in more effective risk management [47]. Therefore, the equation in determining the value of alpha cut of T2FEMD based on Figure 2 can be given as follows.

$$\alpha^{c} = \frac{1}{6}\left(aa_i + F_i + dd_i + bb_i + F_i + cci\right) \tag{4}$$

Intuitionistic fuzzy numbers (IFNs) play a significant role in enhancing the precision of alpha-cut determination following the establishment of the initial alpha value, which is derived from the centroid of a triangular T2FN. Utilizing the centroid approach to determine the center of mass or the average of the triangular area, the subsequent step involves refining this alpha value by incorporating the membership and non-membership degrees related to intuitionistic fuzzy sets. Prakash et al. [48] indicate that this refined alpha value effectively addresses uncertainty in both membership and non-membership directions. The incorporation of intuitionistic fuzzy set properties allows researchers to achieve a deeper comprehension of fuzzy data, resulting in more significant alpha-cut intervals. This dual representation enables a thorough analysis that accounts for the inherent uncertainty and variability in measurements, thereby offering a solid framework for future risk assessments and decision-making processes.

Furthermore, when researchers calculate alpha-cuts using intuitionistic fuzzy numbers, they successfully convert the intricate relationships among various fuzzy values into manageable intervals, facilitating a systematic analysis of uncertainty levels [49, 50] . When a T2FN produces an alpha value indicating uncertainty regarding a set of measurements, utilizing the intuitionistic fuzzy framework provides a more comprehensive understanding of how variations might influence results. The capacity to visualize both membership and non-membership within specified alpha levels demonstrates the effectiveness of intuitionistic fuzzy numbers in tackling associated challenges in areas like seismic data modeling [46]. Through the application of algorithms that integrate the alpha-cut method with intuitionistic fuzzy principles, researchers are able to develop more sophisticated predictive models. These models improve both the accuracy and interpretability of data in environments characterized by uncertainty, thereby promoting enhanced readiness for potential risks and hazards .

Definition 3.4

Let X be universe of discourse. An intuitionistic fuzzy set, $\hat{A}$ in X is defined as:

$$\hat{A} = \left\{ \left\langle x, \mu_{\hat{A}}(x), \nu_{\hat{A}}(x) \right\rangle \middle| x \in X \right\} \tag{5}$$

where $\mu_{\hat{A}}(x) \in [0,1]$ and $\nu_{\hat{A}}(x) \in [0,1]$ are the membership and non membership degree of x in $\hat{A}$ repectively which $0 \le \mu_{\hat{A}}(x) + \nu_{\hat{A}}(x) \le 1$ [51].

Definition 3.5

An intuitionistic fuzzy number (IFN), $\hat{A}^{R}$ is defined as:

$$\hat{A}^{R} = \left\{ \left\langle x, \mu_{\hat{A}^{R}}(x), \nu_{\hat{A}^{R}}(x) \right\rangle \middle| x \in {}^{\sim} \right\} \tag{6}$$

where $\hat{A}^{R} = \left\{ \left\langle x, , \nu_{\hat{A}^{R}}(x) \right\rangle \middle| x \in {}^{\sim} \right\}$ $\mu_{\hat{A}^{R}}(x) : {}^{\sim} \to [0,1]$ and $\nu_{\hat{A}^{R}}(x) : {}^{\sim} \to [0,1]$ represent the membership and non-membership degrees which $0 \le \mu_{\hat{A}^{R}}(x) + \nu_{\hat{A}^{R}}(x) \le 1$ with the hesitation degree is $\pi_{\hat{A}^{R}}(x) = 1 - \mu_{\hat{A}^{R}}(x) - \nu_{\hat{A}^{R}}(x)$ [51, 52].

Definition 3.6

Let A be an intuitionistic fuzzy set (IFS) defined on a universe $\sim$ where:

$$\hat{A}^R = \left\{ \left\langle x, \mu_{\hat{A}^R}(x), \nu_{\hat{A}^R}(x) \right\rangle \middle| x \in {}^{\sim} \right\} \tag{7}$$

Given two threshold $\alpha, \beta \in [0,1]$ such that $\alpha + \beta \leq 1$, intuitionistic alpha-cut defined as:

$$\hat{A}^R_{\alpha,\beta} = \left\{ x \in {}^{\sim} \middle| \mu_{\hat{A}^R} \geq \alpha \text{ and } \nu_{\hat{A}^R} \leq \beta \right\} \tag{8}$$

For type IFN such as triangular IFN, $\hat{A}^R$, then the measurement of membership value $\mu\left(\hat{A}^R\right)$ can be given through Eqn. 9 as follows.

$$\mu\left(\hat{A}^R\right) = \frac{1}{4}\left(a_1 + 2a_2 + a_3\right) \tag{9}$$

Similarly, the measure of non-membership value $\nu\left(\hat{A}^R\right)$ is given by Eqn. 10 as follows

$$v\left(\hat{A}^R\right) = -\frac{1}{4}\left(a_1^{'} + 2a_2^{'} + a_3^{'}\right) \tag{10}$$

Next, the degree of hesitancy and the intuitionistic alpha value can be given by Eqn. 11 and Eqn. 12 respectively.

$$\pi_{\hat{A}^R}\left(a_{ij}\right) = 1 - \mu\left(\hat{A}^R\right) - v\left(\hat{A}^R\right) \tag{11}$$

$$\alpha_{\hat{A}^R} = \mu\left(\hat{A}^R\right) + \pi_{A^R}\left(a_{ij}\right)\mu\left(\hat{A}^R\right) \tag{12}$$

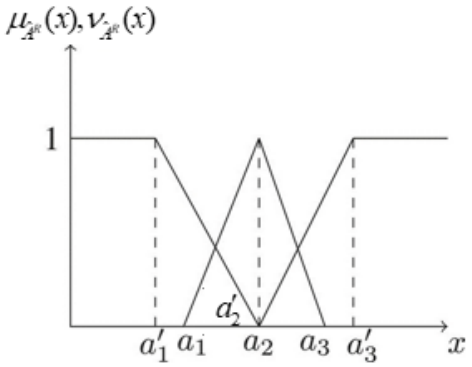

Fig. 4. Triangular intuitionistic alpha-cut

Fig. 4 illustrates the intuitionistic alpha-cut for a triangular IFN as described in Definition 3.6, emphasizing both the membership function, $\mu_{\hat{A}^R}(x)$ and the non-membership function, $\nu_{\hat{A}^R}(x)$ throughout domain x. The triangular shapes demonstrate the graded transition of these functions, with the membership function decreasing from 1 to 0 and then increasing back to 1, while the non-membership function exhibits an inverse pattern. The points a_1, a_2, a_3 denote the critical breakpoints of the triangular membership function, whereas a_1', a_2', a_3' (implicitly aligned) relate to the non-membership curve. The vertical dashed lines define the boundaries set by the second alpha value,

indicating the interval where $\mu_{\hat{A}^R}(x) \geq \alpha$ and $\nu_{\hat{A}^R}(x) \leq \beta$, inline with the condition $\alpha + \beta \leq 1$. The alpha-cut operation generates a subinterval of x values that adhere to the membership and non-membership constraints. The membership value $\mu\left(\hat{A}^R\right)$, non-membership value $\nu\left(\hat{A}^R\right)$, degree hesitancy $\pi_{\hat{A}^R}$, and intuitionistic alpha value $\alpha_{\hat{A}^R}$ can be determined from this subset using Eq. (9)–(12).

Based on Definition 3.3, when IFN implemented, then the process of alpha-cut process is also the same where the different that is the alpha value, first alpha value, and second alpha value (where the IFN been applied). Note that, first alpha value will determined through Eq. (4). Then, the second alpha value will be implemented when first alpha value determined along together Eq. (4). Therefore, the representative symbols for both alpha values can be defined as α^C and $\hat{\alpha}^C$ are alpha cut value for the first and second alpha values respectively.

The implementation of alpha-cuts in T2FEMD is a critical procedure for minimizing the FOU at a designated confidence level alpha. The execution of the alpha-cut operation on both the outer and inner membership functions of the T2FEMD effectively narrows the broad uncertainty interval into a more precise range, while preserving the fundamental uncertainty characteristics of the original data. This process entails linearly interpolating between the peak magnitude value E_i and the left $\left(aa_i, bb_i\right)$ and right $\left(cc_i, dd_i\right)$ support points. This results in the reduced intervals $\left[aa_{i_\alpha}, bb_{i_\alpha}\right]$ and $\left[cc_{i_\alpha}, dd_{i_\alpha}\right]$ for the selected alpha-level. This alpha-cut refinement enhances the clarity of uncertainty visualization across various confidence thresholds and facilitates subsequent analytical operations such as intuitionistic processing, defuzzification or comparative analysis on a more focused and pertinent subset of the magnitude data.

However, if the chosen alpha value in the T2FEMD displays both partial truth and partial falsity, this suggests that the membership information alone is inadequate for reaching a definitive conclusion. In these scenarios, a framework employing IFN can be utilized to efficiently handle the degree of membership (μ), the degree of non-membership (ν), and the degree of hesitancy (π). The initial alpha-cut from the T2FEMD is utilized to improve the FOU in alignment with the membership function. The subsequent interval is assessed within the IFN framework to ascertain a secondary alpha value that takes into account both truth and falsity constraints, guaranteeing that $\alpha + \beta \leq 1$. This dual-stage alpha-cut approach enhances the decision-making process where the type-2 fuzzy model addresses uncertainty in magnitude measurement, while the intuitionistic fuzzy layer manages ambiguity arising from incomplete or conflicting information, leading to a more balanced and reliable range for earthquake magnitude assessment.

The dual-stage alpha-cut process initiates with T2FEMD and is further enhanced through the application of an IFN. This approach yields a more succinct and reliable interval that adeptly incorporates the degrees of truth, falsity, and hesitancy, thereby representing earthquake magnitude with enhanced confidence. After acquiring this refined interval, the next essential step is type-reduction, in which the T2FS is transformed into a suitable type-1 fuzzy set by incorporating all possible embedded fuzzy sets within the specified alpha-cut interval. This process effectively consolidates the FOU into a single fuzzy representation, enabling more straightforward defuzzification or additional analysis. In this context, type-reduction serves as the link between the complex, uncertainty T2FEMD and tangible numerical results. The operation is characterized as the procedure that converts a T2FS into a type-1 fuzzy set by determining its centroid or an alternative representative value across all permissible secondary memberships. Then, the type-reduction can be defined as Definition 3.7 as follows.

Definition 3.7

Let $\tilde{\tilde{E}}_i$ be a set T2FEMD and $\tilde{\tilde{E}}_{i_{\hat{\alpha}^c}}$ are the set of T2FEMD after the alpha-cut process for $i = 0,1,2,..,n$, then the type-reduction of $\tilde{\tilde{E}}_{i_{\hat{\alpha}^c}}$ which is represented as $\tilde{\tilde{E}}^{TR}_{i_{\hat{\alpha}^c}}$ can be defined as follows

$$\tilde{\tilde{E}}^{TR}_{\hat{\alpha}^c} = \left\{ \tilde{\tilde{E}}^{TR}_{i_{\hat{\alpha}^c}} = \left\langle a^{TR}_{i_{\hat{\alpha}^c}}, E_i, b^{TR}_{i_{\hat{\alpha}^c}} \right\rangle \middle| i = 0,1,2,...,n \right\}$$

(12)

where E_i is crisp data points and $a^{TR}_{i_{\hat{\alpha}^c}}$ and $b^{TR}_{i_{\hat{\alpha}^c}}$ are left and right type-reduced alpha-cut T2FEMD respectively with their formulation given by

$$a^{TR}_{i_{\hat{\alpha}^c}} = \frac{1}{2} \sum_{i=0,1,...,n} \left\langle aa_{i_{\hat{\alpha}^c}} + bb_{i_{\hat{\alpha}^c}} \right\rangle$$

$$b^{TR}_{i_{\hat{\alpha}^c}} = \frac{1}{2} \sum_{i=0,1,...,n} \left\langle cc_{i_{\hat{\alpha}^c}} + dd_{i_{\hat{\alpha}^c}} \right\rangle$$

(13)

Definition 3.7 describes the type-reduction process for a set of T2FEMD following the alpha-cut and where applicable, the subsequent alpha-cut through the refinement of IFN. The type-reduced set $\tilde{\tilde{E}}^{TR}_{i_{\hat{\alpha}^c}}$ is characterized by its left $\left(a^{TR}_{i_{\hat{\alpha}^c}}\right)$and right $\left(b^{TR}_{i_{\hat{\alpha}^c}}\right)$ boundaries, which are established as the average of the corresponding left-left/right-left and left-right/right-right alpha-cut points. This operation incorporates the residual FOU into a type-1 fuzzy interval, maintaining the fundamental characteristics of the original type-2 fuzzy data while enhancing it for subsequent processing. Following the completion of the type-reduction step, the subsequent phase is defuzzification, during which the type-1 fuzzy interval is transformed into a single crisp value which commonly employing techniques such as the centroid calculation to facilitate accurate numerical interpretation and informed decision-making based on the earthquake magnitude data. Then, Definition 3.8 will be defined as a defuzzification process as given as follows.

Definition 3.8

Let $\tilde{\tilde{E}}^{TR}_{i_{\hat{\alpha}^c}}$ be the type-reduction alpha-cut T2FEMD with $i = 0,1,2,...,n$. Then, $\tilde{\tilde{E}}^{D}_{i_{\hat{\alpha}^c}}$ is defuzzification process of $\tilde{\tilde{E}}^{TR}_{i_{\hat{\alpha}^c}}$ if for every $\tilde{\tilde{E}}^{TR}_{i_{\hat{\alpha}^c}} \in \tilde{\tilde{E}}^{TR}_{\hat{\alpha}^c}$,

$$\tilde{\tilde{E}}^{D}_{\hat{\alpha}^c} = \left\{ \tilde{\tilde{E}}^{D}_{i_{\hat{\alpha}^c}} \middle| i = 0,1,2,...,n \right\}$$

(14)

where for each $\tilde{\tilde{E}}^{D}_{i_{\hat{\alpha}^c}}$ can be formalized as

$$\tilde{\tilde{E}}^{D}_{i_{\hat{\alpha}^c}} = \frac{1}{3} \sum_{i=0,1,...,n} \left\langle a^{TR}_{i_{\hat{\alpha}^c}}, E_i, b^{TR}_{i_{\hat{\alpha}^c}} \right\rangle$$

(15)

Definition 3.8 describes the defuzzification stage applied to the type-reduced alpha-cut T2FEMD. Once type-reduction has been performed, yielding the interval $\left(a_{i_{\hat{\alpha}^C}}^{TR}, E_i, b_{i_{\hat{\alpha}^C}}^{TR}\right)$ for each data point, defuzzification converts this interval into a single crisp value. The process is defined for the set $\overleftrightarrow{E}_{\hat{\alpha}^C}^{D}$, where each element $\overleftrightarrow{E}_{i_{\hat{\alpha}^C}}^{D}$ is computed as the average of the left type-reduced bound $a_{i_{\hat{\alpha}^C}}^{TR}$, the crisp magnitude E_i, and the right type-reduced bound $b_{i_{\hat{\alpha}^C}}^{TR}$, divided by 3 as Eq. (15). This produces a precise numerical representation of the earthquake magnitude while retaining the influence of the uncertainty boundaries obtained from the type-2 fuzzy modeling process. Essentially, defuzzification finalizes the transformation from the original fuzzy, uncertain data into a single actionable magnitude value suitable for interpretation, reporting, and decision-making.

The type-2 fuzzy interpolation Bézier curve (T2FIBC) is an advanced mathematical modeling technique designed to represent and approximate data characterized by uncertainty, imprecision, and vagueness, particularly in situations where type-1 fuzzy models do not fully capture the entire spectrum of variability. This method integrates the geometric adaptability of Bézier curves with the functionalities of T2FSs, enabling seamless and continuous interpolation among type-2 fuzzy control points, while preserving the FOU along the curve. In this context, each control point is defined as a T2FN, ensuring that the resulting curve not only interpolates the given data but also incorporates the related uncertainty at each position along its path. The methodology for T2FIBC is an essential instrument for modeling real-world datasets, such as earthquake magnitude records, shoreline changes, and hydrological flows. The methodology thoroughly addresses measurement errors, data incompleteness, and inherent variability, ensuring that both the shape and the uncertainty profile of the modeled curve are meticulously evaluated. Therefore, the next definition is the defining the T2FIBC piecewisely curve.

Definition 3.9

Given T2FEMD, $\overleftrightarrow{E}_i$ and type-2 fuzzy derivative values at t, $\overleftrightarrow{D}_i$ where $\overleftrightarrow{D}_i, \overleftrightarrow{E}_i \in \tilde{}$, $i = 0,1,...,n$. Then, the type-2 fuzzy interpolation Bezier curve can be defined as

$$\overleftrightarrow{B}(t) = (1-t)^3 \overleftrightarrow{E}_i + 3t(1-t)^2 \overleftrightarrow{K}_i + 3t^2(1-t)\overleftrightarrow{L}_i + t^3 \overleftrightarrow{E}_{i+1}$$

(16)

with

$$\overleftrightarrow{K}_i = \frac{\overleftrightarrow{D}_i}{3} + \overleftrightarrow{E}_i$$

$$\overleftrightarrow{L}_i = \overleftrightarrow{E}_{i+1} - \frac{\overleftrightarrow{D}_{i+1}}{3}$$

(17)

such that $\overleftrightarrow{D}_i$ and $\overleftrightarrow{D}_{i+1}$ are type-2 tangent vector of T2FEMD where the representation of the type-2 fuzzy tangent values can be given as follows.

$$\overleftrightarrow{D}_0 = 2\left(\overleftrightarrow{E}_1 - \overleftrightarrow{E}_0\right) - \frac{\left(\overleftrightarrow{E}_2 - \overleftrightarrow{E}_0\right)}{2},$$

(18)

$$\ddot{\ddot{D}}_n = 2\left(\ddot{\ddot{E}}_n - \ddot{\ddot{E}}_{n-1}\right) - \frac{\left(\ddot{\ddot{E}}_n - \ddot{\ddot{E}}_{n-2}\right)}{2},$$

(19)

$$\ddot{\ddot{D}}_i = h_i\left(\ddot{\ddot{E}}_i - \ddot{\ddot{E}}_{n-1}\right) + \left(1-h_i\right)\left(\ddot{\ddot{E}}_{i+1} - \ddot{\ddot{E}}_i\right)$$

(20)

where

$$h_i = \frac{\left\|\ddot{\ddot{E}}_{i+1} - \ddot{\ddot{E}}_i\right\|}{\left\|\ddot{\ddot{E}}_{i+1} - \ddot{\ddot{E}}_i\right\| + \left\|\ddot{\ddot{E}}_i - \ddot{\ddot{E}}_{i-1}\right\|}$$

(21)

for $i = 1, 2, .., n-1.$

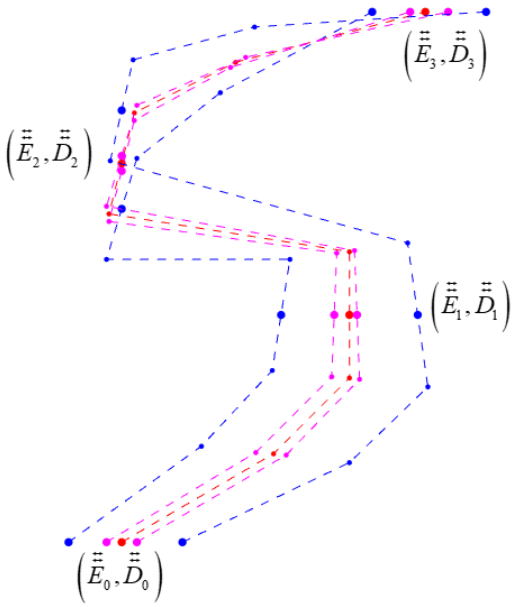

Fig. 4. Type-2 fuzzy control polygon consists of type-2 fuzzy tangent vector and T2FEMD

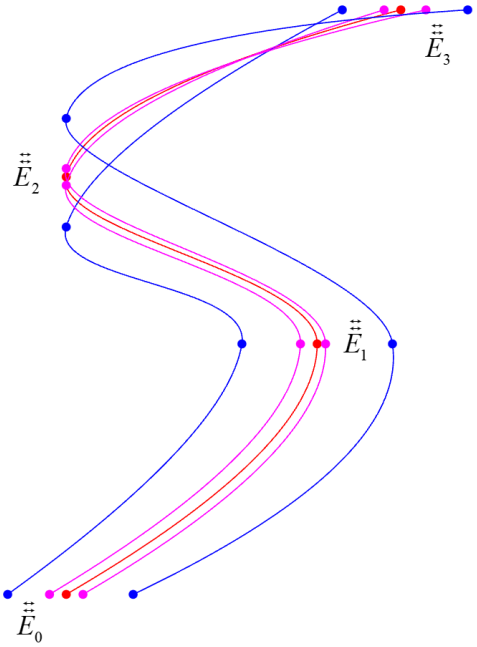

Fig. 5. T2FIBC interpolate all T2FEMD, $\ddot{\ddot{E}}_0, \ddot{\ddot{E}}_1, \ddot{\ddot{E}}_2$ and $\ddot{\ddot{E}}_3$.

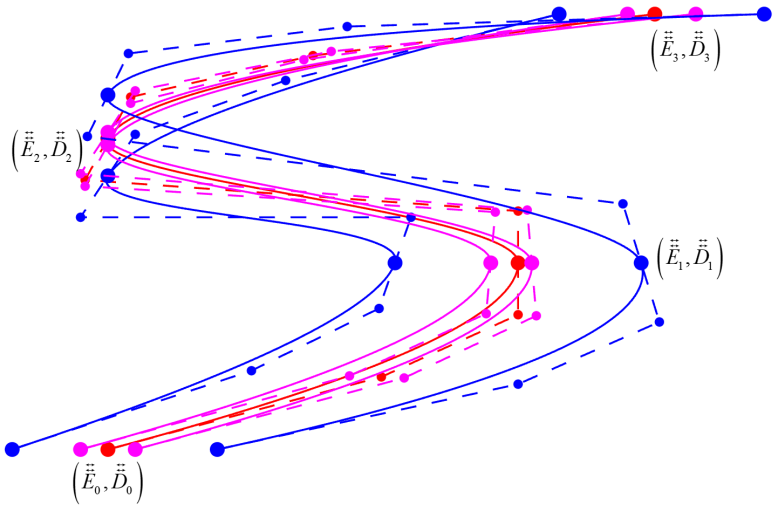

Fig. 6. T2FIBC interpolates all T2FEMD together with the type-2 fuzzy control polygon and the type-2 fuzzy tangent vector

Figure 4-6 illustrate the process of creating the T2FIBC and addressing the gaps within it to obtain T2FEMD. Figure 4 illustrates the type-2 fuzzy control grid. The blue dashed lines indicate the fuzzy control points $\left(\ddot{\ddot{E}}_i, \ddot{\ddot{D}}_i\right)$. The dashed magenta tangent vectors link each point and indicate a specific direction, regardless of any uncertainties that may arise. Figure 5 illustrates the functionality of the interpolation technique. This section illustrates the seamless movement of the T2FIBC around the fuzzy areas E_0, E_1, E_2 and E_4 at the center. The blue and purple lines represent the maximum and minimum values that the type-2 fuzzy membership functions can offer. Figure 6 presents the adjusted curves, a type-2 fuzzy control polygon along with the associated tangent vectors. This encompasses the entire model. This illustrates the relationship between fuzzy uncertainty and geometric configuration. This ensures that information regarding earthquake magnitudes, which may lack clarity is communicated reliably and consistently. The transition from control polygons to integrated

curve analysis demonstrates the effectiveness of the T2FIBC approach in monitoring data trends and rectifying errors in seismic data modeling.

3.1 Type-2 Fuzzy Interpolation Bezier Curve of Earthquake Magnitude Data at Ranau, Sabah

In 2017, Ranau, Sabah, recorded a notable occurrence of earthquakes, amounting to 55 throughout the year. The occurrence of earthquakes in the region indicates a significant likelihood of future events. This can be largely ascribed to its location within a dynamic tectonic zone linked to the Ring of Fire. Ranau is at risk of earthquakes as a result of its geological characteristics, shaped by local fault systems and regional tectonic activity. The local infrastructure was developed with inadequate consideration for seismic activity, rendering it vulnerable to potential damage. This highlights the importance of improving the earthquake resilience of structures in the region.

The earthquake that occurred in Ranau on June 5, 2015, with a moment magnitude of 6.0, underscores the considerable effects that seismic events can impose on the region. Subsequent to the earthquake, further calamities transpired, encompassing landslides and rockfalls across multiple areas. This demonstrates the relationships between geological hazards. The occurrence of 55 earthquakes in 2017 highlights the importance of monitoring earthquake risk and conducting research to accurately quantify and manage it. This comprehensive strategy will be crucial for addressing risks and assessing the vulnerabilities of both individuals and infrastructure in Ranau and its surrounding areas.

The interconnected nature of geological hazards highlights the importance of ongoing seismic monitoring, comprehensive hazard assessment, and effective mitigation strategies to protect lives and infrastructure. In this context, advanced modeling techniques, including the piecewise T2FIBC, serve as crucial instruments for effectively capturing the uncertainty in earthquake magnitude data. This enhances risk assessment and facilitates informed decision-making for disaster preparedness in Ranau and its neighboring regions.

This study will focus on selecting a subset of 20 earthquake magnitude data points from the total of 55 recorded events in Ranau, Sabah, for preliminary analysis. This approach is mainly influenced by computational limitations, as managing all 55 data points at once could result in performance delays during the modeling phase. The selection of 20 data points enables thorough testing and validation of the proposed methodology, while also optimizing the use of computational resources. Following the successful execution of the analysis for the 20 data points, the current modeling framework can be effectively utilized for all 55 data points without requiring any methodological adjustments. Furthermore, the 20 selected data points represent a suitable subset of the entire dataset, allowing the results achieved to provide a reliable initial evaluation of the model's performance. This will enable a smooth transition to a more thorough analysis once computational constraints are resolved. Therefore, based on Definition 3.9 and the T2FEMD of Ranau Earthquake Magnitude Data, then the T2FIBC of those data can be modeled and visualized as follows.

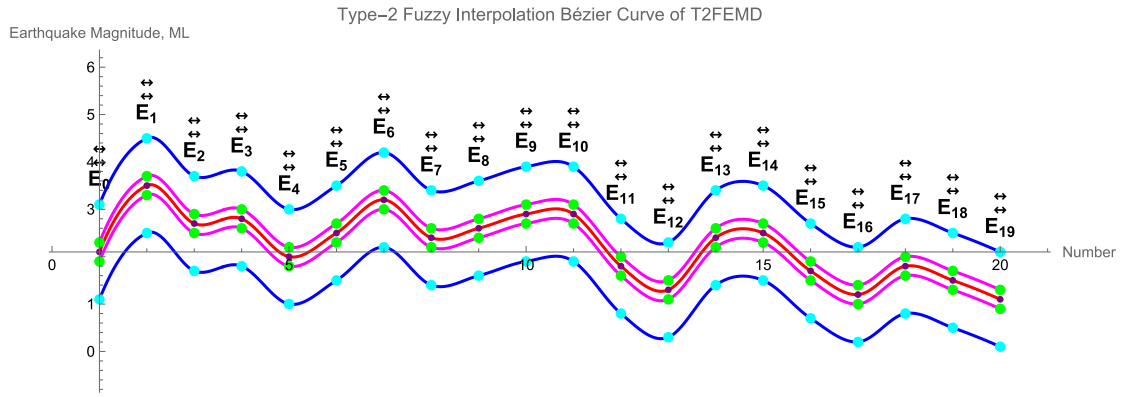

Fig. 7. Piecewise cubic type-2 fuzzy interpolation Bezier curve of T2FEMD

Figure 7 presents the piecewise cubic T2FIBC created from the T2FEMD for Ranau, Sabah, employing 20 selected data points as fuzzy control points. Each point, referred to as $\tilde{\tilde{E}}_i$, is linked to a type-2 fuzzy uncertainty, characterized by the FOU, which is delineated by the upper and lower membership functions. The cubic Bézier segments effectively link these points providing a smooth representation of variations in earthquake magnitude, while the various embedded curves illustrate distinct membership grades within the FOU. This approach preserves the dataset's continuity and its uncertainty characteristics, enabling a realistic and interpretable visualization of the magnitude range.

Upon completion of the T2FIBC construction, the subsequent step involves employing the alpha-cut procedure to derive the interval of the T2FS at a specified membership grade (α). This simplifies the representation while maintaining the uncertainty information. The intuitionistic alpha value assists individuals in decision-making when the data presents both true and false information. The values of membership $\mu\left(\hat{A}^R\right)$ and non-membership $\nu\left(\hat{A}^R\right)$ are initially established through the parameters of the triangular IFN $\left(a_1, a_2, a_3\right)$, as demonstrated in Eq. (9)-(12). The degree of hesitancy $\pi_{\hat{A}^R}$ represents the level of uncertainty that remains after considering both membership and non-membership factors. The intuitionistic alpha value $\alpha_{\hat{A}^R}$ is determined by summing the membership value with the adjusted membership value that accounts for reluctance. This illustrates the degree of certainty and hesitation inherent in the decision-making process. The improved alpha value ensures that the fuzzy intervals derived from the alpha-cut process accurately represent the uncertainty and reluctance inherent in earthquake magnitude data. The subsequent type-reduction and defuzzification processes are rendered more reliable as a result.

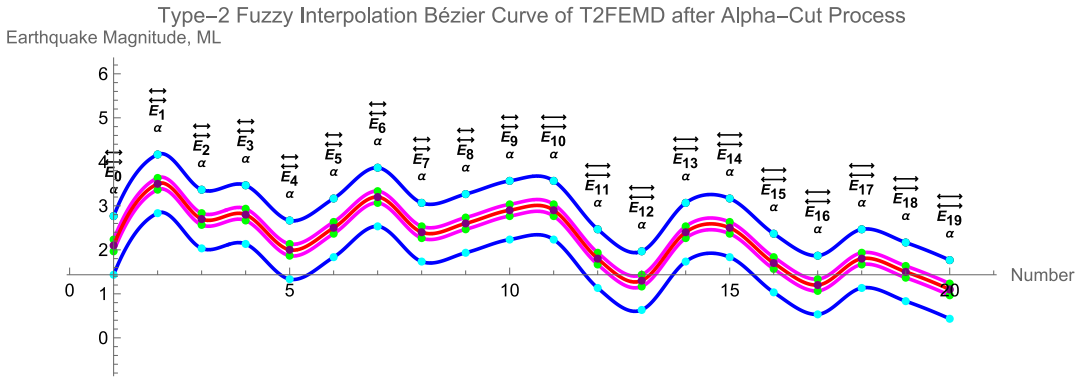

Fig. 8. Piecewise cubic type-2 fuzzy interpolation Bezier curve of T2FEMD after alpha-cut process

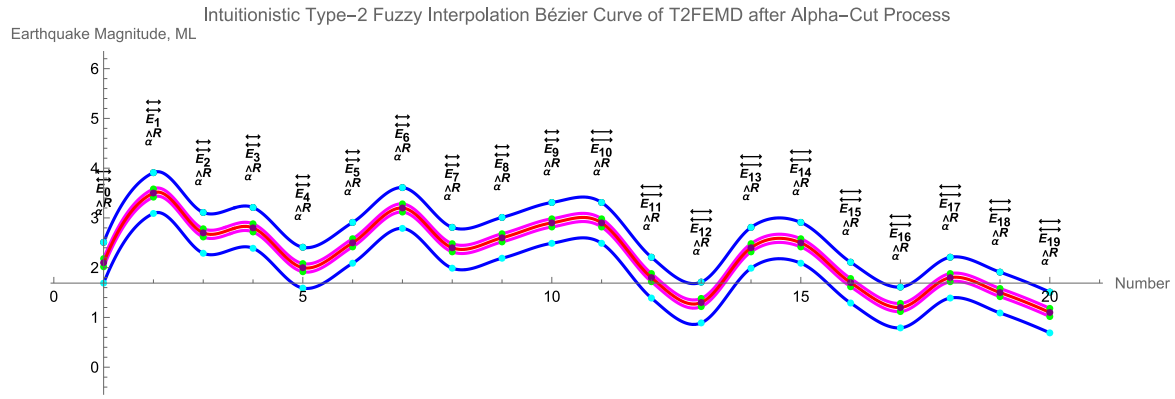

Fig. 9. Piecewise cubic intuitionistic type-2 fuzzy interpolation Bezier curve of T2FEMD after second alpha-cut process

Following the application of the alpha-cut method with α=0.3333, Fig. 8 illustrates the piecewise cubic T2FIBC derived from the T2FEMD. At this alpha level, each type-2 fuzzy data point is converted into an interval type-1 fuzzy set. This maintains the uncertainty range defined by the FOU while excluding membership grades that fall below the threshold. Figure 9 illustrates the T2FIBC following the alpha-cut procedure, utilizing an intuitionistic alpha value of 0.59. The value was determined by summing the degrees of membership, non-membership, and hesitation as outlined in Eq. (9)-(12). The curve presented in Figure 9 illustrates a more precise and detailed uncertainty band compared to that in Figure 8. The intuitionistic alpha value considers hesitation, resulting in a more balanced interval width that accurately reflects the dual nature of the data as both true and false.

After completing the alpha-cut and intuitionistic alpha-cut stages, the subsequent step in the processing of the T2FIBC model is the type-reduction process. This step involves converting interval T2FSs into a type-1 fuzzy set by aggregating the upper and lower membership boundaries. This step is essential as it converts the complex type-2 representation into a format appropriate for final defuzzification, while preserving the effects of uncertainty captured in the earlier stages. Different type-reduction methods, including the Karnik–Mendel (KM) algorithm and improved iterative procedures, can be utilized to ascertain the centroid of the reduced set. This guarantees that the resulting type-1 representation precisely captures the variability and uncertainty inherent in the original T2FEMD.

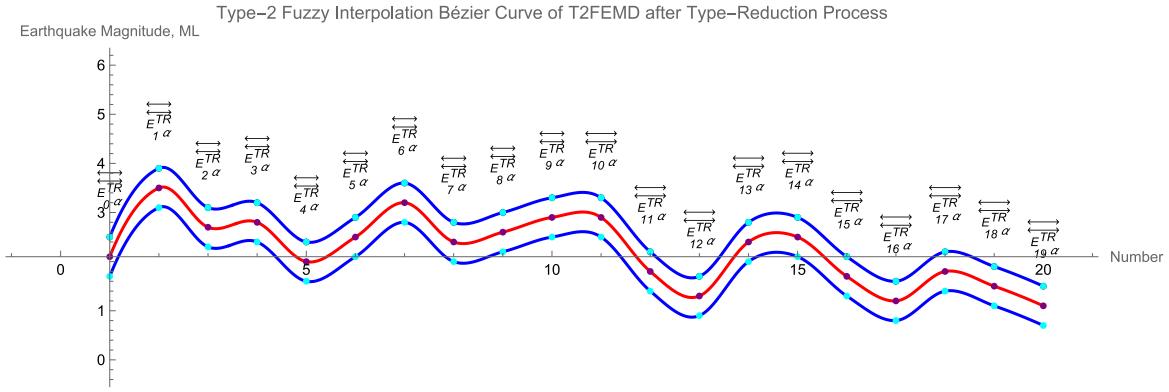

Fig. 10. Piecewise cubic type-2 fuzzy Interpolation Bezier curve after type-reduction process

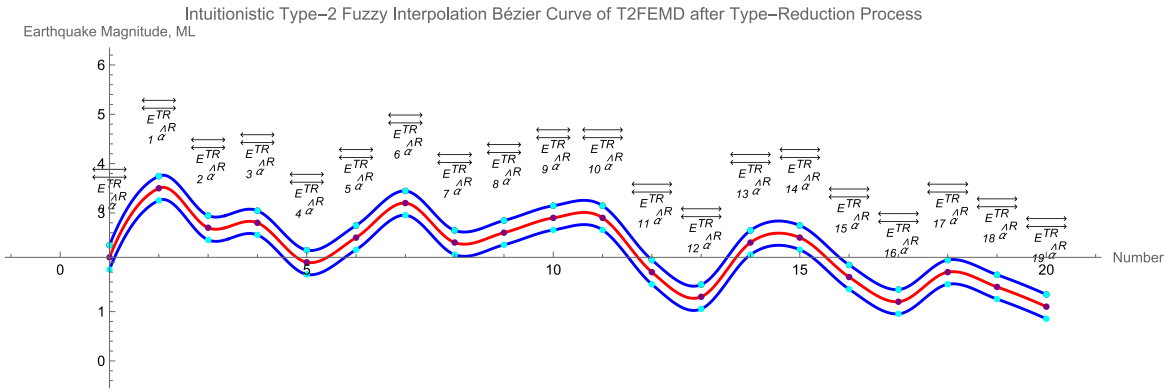

Fig. 11. Piecewise cubic intuitionistic type-2 fuzzy interpolation Bezier curve after second type-reduction process

Figure 10 illustrates the piecewise cubic T2FIBC of the T2FEMD following the type-reduction process. The curve demonstrates the process of converting the transformed T2FS into a type-1 fuzzy set by aggregating the upper and lower membership boundaries, while preserving the uncertainty distribution recognized during the alpha-cut phase. The blue and red boundary curves represent the FOU, while the central black line indicates the centroid-based reduced type-1 set. Figure 11 presents the piecewise cubic intuitionistic T2FIBC which adheres to the second type-reduction process and incorporates the intuitionistic alpha value. This results in an improved model representation that integrates both membership and non-membership information, thus enabling a more precise depiction of the uncertainty distribution inherent in the original T2FEMD data.

Following type-reduction, the subsequent essential step is defuzzification, which transforms the reduced type-1 fuzzy set into a precise numerical value appropriate for interpretation and decision-making. Various defuzzification methods, including the centroid of area (COA), weighted average, or mean of maxima, can be utilized based on the specific modeling objective. This step concludes the uncertainty modeling process by producing a singular representative value from the fuzzy domain, while preserving the impact of the preceding fuzzy and intuitionistic phases. The final output is guaranteed to be mathematically valid and pertinent for future analyses or applications.

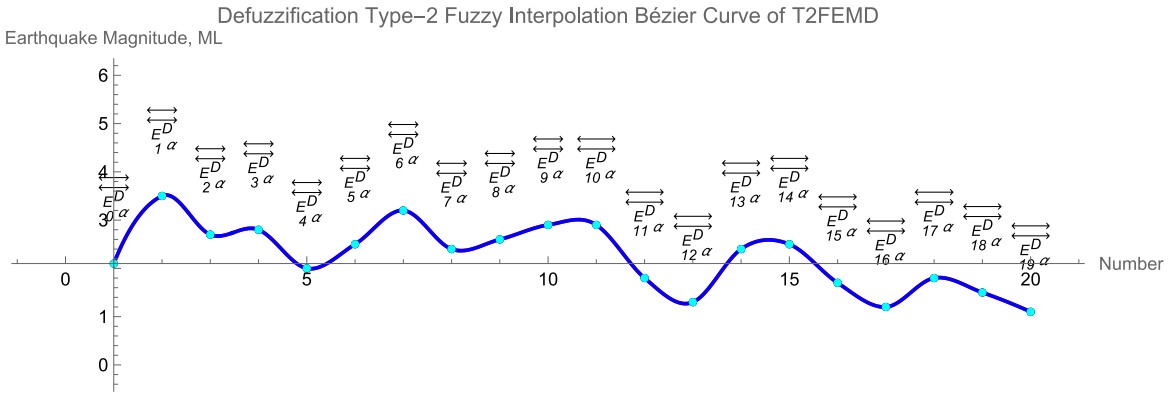

Fig. 12. Piecewise cubic type-2 fuzzy Interpolation Bezier curve after defuzzification process

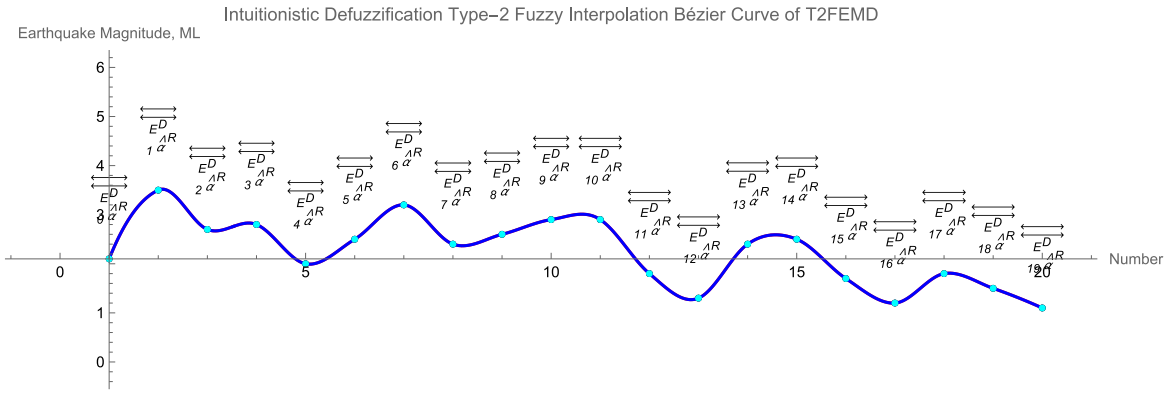

Fig. 13. Piecewise cubic intuitionistic type-2 fuzzy interpolation Bezier curve after defuzzification process

Figure 12 illustrates the piecewise cubic T2FIBC of T2FEMD following the defuzzification process, in which the previously type-reduced fuzzy set is converted into a singular crisp curve. The blue curve illustrates the final precise magnitude estimation derived from the centroid of the aggregated type-1 set, accurately reflecting the core trend while removing the fuzzy spread. Figure 13 illustrates the piecewise cubic intuitionistic T2FIBC following defuzzification, which integrates both membership and non-membership degrees derived from the intuitionistic alpha-cut stage. This generates a polished and precise curve that considers a broader range of uncertainties, which may result in more accurate and context-sensitive magnitude assessments.

The subsequent step involves performing a comparative analysis between the defuzzified curve and the original T2FEMD curve, in addition to the defuzzified intuitionistic curve and the original. This analysis assesses the effectiveness of the specific outputs in maintaining the integrity of the original shape, peak positions, and magnitude values, while also striving to minimize uncertainty. Through the analysis of deviations, error metrics, and visual alignment, one can evaluate if the integration of intuitionistic information offers a notable enhancement compared to the conventional defuzzification process. This step is essential for confirming the effectiveness and reliability of both methods in accurately representing real-world earthquake magnitude data.

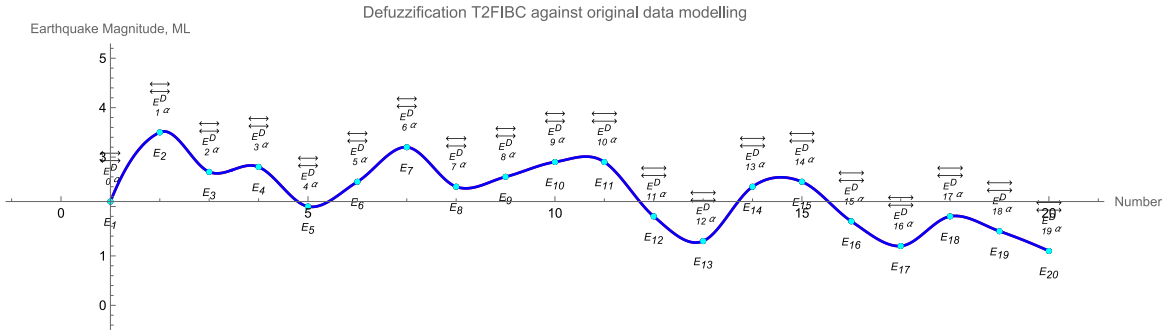

Fig. 14. Defuzzified Type-2 Fuzzy Interpolation Bezier Curve model against crisp interpolation Bezier curve model

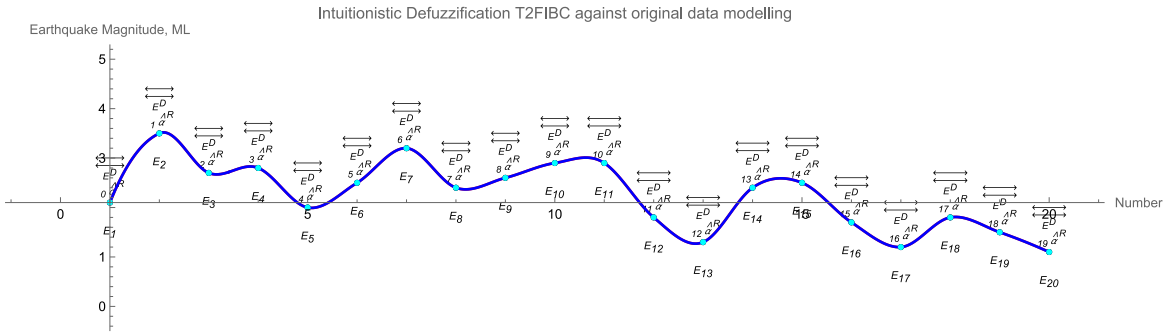

Fig. 15. Defuzzified Intuitionistic Type-2 Fuzzy Interpolation Bezier Curve model against crisp interpolation Bezier curve model

Figure 14 presents the defuzzified T2FIBC in comparison to the original crisp interpolation Bézier curve model. The blue defuzzified curve closely aligns with the shape and peaks of the original data trend. The visual alignment indicates that the type-2 fuzzy defuzzification process successfully maintains the key characteristics of the original curve while removing the fuzziness from prior stages. Figure 15 illustrates the defuzzified intuitionistic T2FIBC, alongside a comparison to the crisp interpolation curve. The incorporation of intuitionistic parameters, which account for both membership and non-membership degrees, enhances the curve fitting process, providing a more precise alignment with the original crisp data, even though the plotted graphs exhibit only slight visible differences.

Table 1
Comparison between crisp, defuzzified and defuzzified intuitionistic of T2FEMD

Crisp Earthquake Magnitude Data	Defuzzified T2FEMD	Defuzzified Intuitionistic T2FEMD
(1,2.1)	(1,2.1)	(1,2.1)
(2,3.5)	(2,3.5)	(2,3.5)
(3,2.7)	(3,2.7)	(3,2.7)
(4,2.8)	(4,2.8)	(4,2.8)
(5,2.0)	(5,2.0)	(5,2.0)
(6,2.5)	(6,2.5)	(6,2.5)
(7,3.2)	(7,3.2)	(7,3.2)
(8,2.4)	(8,2.4)	(8,2.4)
(9,2.6)	(9,2.6)	(9,2.6)
(10,2.9)	(10,2.9)	(10,2.9)
(11,2.9)	(11,2.9)	(11,2.9)
(12,1.8)	(12,1.8)	(12,1.8)
(13,1.3)	(13,1.3)	(13,1.3)
(14,2.4)	(14,2.4)	(14,2.4)
(15,2.5)	(15,2.5)	(15,2.5)
(16,1.7)	(16,1.7)	(16,1.7)
(17,1.2)	(17,1.2)	(17,1.2)
(18,1.8)	(18,1.8)	(18,1.8)
(19,1.5)	(19,1.5)	(19,1.5)
(20,1.1)	(20,1.1)	(20,1.1)

Table 2
Comparison of statisctic perfomance measure between crisp with defuzzified and crisp with defuzzified intuitionistic of T2FEMD

Type of Statistical Perfomance	Crisp with Defuzzified T2FEDM	Crisp with Defuzzified Intuitionistic T2FEMD
Root Mean Square Error (RMSE)	2.32882×10^{-16}	2.32882×10^{-16}
Mean Absolute Error (MAE)	1.33227×10^{-16}	1.33227×10^{-16}
Mean Absolute Percentage Error (MAPE)	5.75299×10^{-15}	5.75299×10^{-15}
Coefficient of Determination (R^2)	1	1

Considering that the plotted curves in Figure 14 and Figure 15 do not clearly demonstrate the subtle differences among the crisp data, defuzzified data, and intuitionistic defuzzified data, a numerical comparison for all data points is regarded as more appropriate. A table can be employed to display each data point, encompassing the crisp value, the defuzzified value, and the defuzzified intuitionistic value, along with their respective differences from the crisp reference as in Table 1. To evaluate the model's effectiveness, it is advisable to compute several statistical performance measures, such as Root Mean Square Error (RMSE), Mean Absolute Error (MAE), Mean Absolute Percentage Error (MAPE), and Coefficient of Determination (R^2). A table can be developed to summarize the comparison between crisp, defuzzified data and intuitionistic defuzzified data which mentioned in Table 2. Lower RMSE, MAE, and MAPE values, combined with higher R^2 scores, would indicate a more accurate model, offering statistical proof to assess whether the intuitionistic defuzzification approach demonstrates a quantifiable improvement over the traditional defuzzification method.

Table 1 presents a point-by-point comparison between the crisp earthquake magnitude data, the defuzzified T2FEMD, and the defuzzified intuitionistic T2FEMD. Each entry lists the index of the data point and its corresponding magnitude values in all three forms. From the table, it is evident that the values for the defuzzified type-2 fuzzy data and the defuzzified intuitionistic type-2 fuzzy data are identical for all 20 points. This indicates that, although the intuitionistic alpha-cut was incorporated in the earlier stages, the subsequent type-reduction and defuzzification steps yielded the same crisp output values as the standard defuzzification method. This can happen if the intuitionistic component does not introduce additional variation at the defuzzification stage which is often due to perfect symmetry between the membership and non-membership functions or because the chosen centroid-based defuzzification method neutralizes the effect of the intuitionistic adjustment.

Table 2 provides a summary of the statistical performance measures that compare (1) the crisp data with the defuzzified T2FEMD and (2) the crisp data with the defuzzified intuitionistic T2FEMD. The metrics include Root Mean Square Error (RMSE), Mean Absolute Error (MAE), Mean Absolute Percentage Error (MAPE), and Coefficient of Determination (R^2). The performance values for both methods are the same, demonstrating exceptionally small error magnitudes (around 10^{-15} to 10^{-16}) and perfect R^2 values of 1, indicating an exact fit. The statistical equivalence noted is a direct consequence of the identical data point values shown in Table 1, thereby reinforcing the conclusion that the intuitionistic extension did not alter the final crisp outputs in this specific case. This outcome

suggests that, under certain conditions, the intuitionistic component may influence uncertainty representation in intermediate fuzzy stages, but does not impact the final defuzzified result.

4. Discussion

The comparative analysis of the earthquake magnitude data, the defuzzified T2FIBC data and the defuzzified intuitionistic T2FIBC data reveals a precise numerical alignment at all evaluated points. The results shown in Table 1 indicate that the intuitionistic alpha-cut method adds an additional phase for handling uncertainty. The crisp values achieved after type-reduction and defuzzification align with those obtained from the traditional T2FIBC method. The observed outcome is linked to the symmetry found in both the membership and non-membership functions along with the attributes of the centroid defuzzification method which effectively addresses any minor variations that may occur during the initial intuitionistic processing.

Table 2 provides statistical measures such as RMSE, MAE, MAPE, and R^2 for assessing model performance through a comparison of the crisp data with the two defuzzification methods. The minimal error values that ranging from 10^{-15} to 10^{-16} and coupled with a R^2 value of 1 demonstrate that both defuzzified datasets closely correspond with the crisp dataset with exceptional precision. This demonstrates that the interpolation and uncertainty modeling framework upholds a significant degree of stability and does not cause numerical distortion during the defuzzification phase, even with the incorporation of the intuitionistic extension.

It is important to acknowledge that although the numerical results are identical, the early stages of the modeling pipeline which particularly during alpha-cut, intuitionistic alpha-cut, and type-reduction where differ in their approach to representing and managing uncertainty. The intuitionistic approach provides a more refined representation by incorporating degrees of hesitation, which can be beneficial in scenarios where uncertainty needs to be evaluated before defuzzification, including decision-making thresholds, multi-criteria evaluations, or risk assessments. In these contexts, the intermediate stages maintain a higher level of detailed uncertainty information in comparison to the standard T2FIBC.

The primary benefit of integrating the intuitionistic approach in this context lies not in altering the final crisp outcomes, but in enhancing the robustness and clarity of the uncertainty representation throughout the intermediate fuzzy phases. This approach improves the method's effectiveness in situations where fuzzy representation is employed for reasoning, rather than relying solely on the final crisp outputs.

5. Conclusion

This work has proven that both the conventional defuzzified T2FIBC model and the defuzzified intuitionistic T2FIBC model can accurately generate crisp earthquake magnitude data with great numerical precision. The modeling framework is stable and accurate since the end findings are always the same and the error metrics are low and the determination coefficients are high.

Adding intuitionistic fuzzy processing does not change the ultimate crisp outputs for the dataset used, but it does improve the intermediate modeling stages by giving them more uncertainty descriptors. This might be helpful in cases when a deep study of uncertainty is needed, even if the final defuzzified numbers don't show these details.

Future studies should look at datasets or application areas where the difference between membership and non-membership functions might cause the two methods to diverge during the

defuzzified stage. Also, looking at other ways to defuzzify outside the centroid approach can show situations where the intuitionistic extension gives different and perhaps more accurate end results.

Acknowledgement
The authors would like to thank the Ministry of Higher Education (MOHE) Malaysia for funding this research under the Fundamental Research Grant Scheme (FRGS) with grant number FRGS/1/2022/STG06/UMS/02/3. We also like to thank Universiti Malaysia Sabah (UMS) in facilitating this research.

References

[1] Zhang, Guo-Fang, Li-Hui He, and Sen Li. "A fuzzy-random optimization approach using fuzzy measure and fuzzy integral for emergency risk coordination of supply chain." In *2014 International Conference on Machine Learning and Cybernetics*, vol. 2, pp. 789-795. IEEE, 2014. https://doi.org/10.1109/icmlc.2014.7009710

[2] Jifrin, Arina Nabilah, Rozaimi Zakaria, and Isfarita Ismail. "Fuzzy intuitionistic alpha cut of b-spline curve interpolation modeling for shoreline island data." *Malaysian Journal of Fundamental and Applied Sciences* 19, no. 5 (2023): 781-790.. https://doi.org/10.11113/mjfas.v19n5.3074

[3] Abel Hailemichael, Syed Moshfeq Salaken, Ali Karimoddini, Abdollah Homaifar, Khosravi Abbas, and Saeid Nahavandi. "Developing a Computationally Effective Interval Type-2 TSK Fuzzy Logic Controller." *Journal of Intelligent & Fuzzy Systems* 38, no. 2 (2019): 1915–1928. https://doi.org/10.3233/jifs-190446

[4] Xin Jiao, Barış Fidan, Ju Jiang, and Mohamed S. Kamel. "Type-2 Fuzzy Adaptive Sliding Mode Control of Hypersonic Flight." *Proceedings of the Institution of Mechanical Engineers Part G Journal of Aerospace Engineering* 233, no. 8 (2017): 2731–2744. https://doi.org/10.1177/0954410017712329

[5] Shuchen Ding, Xianlin Huang, Xiaojun Ban, Hongqian Lu, and Hongyang Zhang. "Type-2 Fuzzy Logic Control for Underactuated Truss-Like Robotic Finger With Comparison of a Type-1 Case." *Journal of Intelligent & Fuzzy Systems* 33, no. 4 (2017): 2047–2057. https://doi.org/10.3233/jifs-161538

[6] Zuzana Janková, Dipak Kumar Jana, and Petr Dostál. "Investment Decision Support Based on Interval Type-2 Fuzzy Expert System." *Engineering Economics* 32, no. 2 (2021): 118–129. https://doi.org/10.5755/j01.ee.32.2.24884

[7] Saad M. Darwish and Ali Hassan Mohammed. "Interval Type-2 Fuzzy Logic to the Treatment of Uncertainty in 2D Face Recognition Systems." *International Journal of Machine Learning and Computing* (2014): 24–30. https://doi.org/10.7763/ijmlc.2014.v4.381

[8] Giovanni Acampora, Daniyal Alghazzawi, Hani Hagras, and Autilia Vitiello. "An Interval Type-2 Fuzzy Logic Based Framework for Reputation Management in Peer-to-Peer E-Commerce." *Information Sciences* 333 (2016): 88–107. https://doi.org/10.1016/j.ins.2015.11.015

[9] Nur Batrisyia Ahmad Azmi, Rozaimi Zakaria, and Isfarita Ismail. "Type-2 Intuitionistic Interpolation Cubic Fuzzy Bézier Curve Modeling Using Shoreline Data." *Malaysian Journal of Fundamental and Applied Sciences* 19, no. 6 (2023): 1131–1141. https://doi.org/10.11113/mjfas.v19n6.3076

[10] Amir Pourabdollah, Christian Wagner, Michael L. Smith, and Ken Wallace. "Real-World Utility of Non-Singleton Fuzzy Logic Systems: A Case of Environmental Management." (2015): 1–8. https://doi.org/10.1109/fuzz-ieee.2015.7338007

[11] Muhammad Saeed and Fatima Razaq. "Foundational Exploration and Key Properties of Refined Intuitionistic Q-Fuzzy Set: A Comprehensive Study on Mathematical Framework and Set-Theoretic Operations." (2024). https://doi.org/10.22541/au.171601006.63158465/v1

[12] Yanxia Wei and Qinghai Wang. "New Distances for Dual Hesitant Fuzzy Sets and Their Application in Clustering Algorithm." *Journal of Intelligent & Fuzzy Systems* 41, no. 6 (2021): 6221–6232. https://doi.org/10.3233/jifs-202846

[13] Chiara Pomare, Kate Churruca, Louise A. Ellis, Janet C. Long, and Jeffrey Braithwaite. "A Revised Model of Uncertainty in Complex Healthcare Settings: A Scoping Review." *Journal of Evaluation in Clinical Practice* 25, no. 2 (2018): 176–182. https://doi.org/10.1111/jep.13079

[14] Rugen Wang, Weimin Li, Tao Zhang, and Qi Han. "New Distance Measures for Dual Hesitant Fuzzy Sets and Their Application to Multiple Attribute Decision Making." *Symmetry* 12, no. 2 (2020): 191. https://doi.org/10.3390/sym12020191
[15] Yilong Jia, Jinhua Mi, Dong Sun, Libing Bai, and Kai Chen. "Reliability Analysis of Systems With Mixed Uncertainties Based on Bhattacharyya Distance and Bayesian Network." *Quality and Reliability Engineering International* 38, no. 7 (2022): 3741–3754. https://doi.org/10.1002/qre.3170
[16] Xin Tao, Jinzhi Lu, DeJiu Chen, and Martin Törngren. "Probabilistic Inference of Fault Condition of Cyber-Physical Systems Under Uncertainty." *Ieee Systems Journal* 14, no. 3 (2020): 3256–3266. https://doi.org/10.1109/jsyst.2020.2965400
[17] Rozaimi Zakaria, Abd Fatah Wahab, and R. U. Gobithaasan. "Fuzzy B-Spline Surface Modeling." *Journal of Applied Mathematics* 2014 (2014): 1–8. https://doi.org/10.1155/2014/285045
[18] Jiawei Li, Robert John, Simon Coupland, and Graham Kendall. "On Nie-Tan Operator and Type-Reduction of Interval Type-2 Fuzzy Sets." *Ieee Transactions on Fuzzy Systems* 26, no. 2 (2018): 1036–1039. https://doi.org/10.1109/tfuzz.2017.2666842
[19] I. Made Mataram and Insan Wijaya. "Monitoring and Control of Liquid Waste Using Fuzzy Logic Based Internet of Things (IoT)." *International Journal of Latest Engineering Research and Applications (Ijlera)* 8, no. 11 (2023): 154–160.https://doi.org/10.56581/ijlera.8.11.154-160
[20] Manyuk Fauzi, Imam Suprayogi, Sigit Sutikno, Ari Sandhyavitri, and Eko Riyawan. "Development of Erosion Risk Map Using Fuzzy Logic Approach." *Matec Web of Conferences* 101 (2017): 04021. https://doi.org/10.1051/matecconf/201710104021
[21] Tomás Eloy Salais-Fierro, Jania Astrid Saucedo-Martínez, Román Rodríguez-Aguilar, and Jose Manuel Vela-Haro. "Demand Prediction Using a Soft-Computing Approach: A Case Study of Automotive Industry." *Applied Sciences* 10, no. 3 (2020): 829. https://doi.org/10.3390/app10030829
[22] Andrzej Żyluk, Konrad Kuźma, Norbert Grzesik, Mariusz Zieja, and J. Tomaszewska. "Fuzzy Logic in Aircraft Onboard Systems Reliability Evaluation—A New Approach." *Sensors* 21, no. 23 (2021): 7913. https://doi.org/10.3390/s21237913
[23] P. Thirunavukarasu, R. Suresh, and W. Lilly Merline. "Introduction to Complex Fuzzy Soft Hypergroup, Complex Fuzzy Soft Hyperring and Complex Fuzzy Soft Hyperideal." *International Journal of Contemporary Mathematical Sciences* 11 (2016): 359–366.https://doi.org/10.12988/ijcms.2016.6634
[24] Rozaimi Zakaria, Abd F. Wahab, and R. U. Gobithaasan. "Type-2 Fuzzy Bezier Curve Modeling." (2013). https://doi.org/10.1063/1.4801232
[25] Rozaimi Zakaria, Abdul Wahab, and R. U. Gobithaasan. "Normal Type-2 Fuzzy Rational B-Spline Curve." *International Journal of Mathematical Analysis* 7 (2013): 789–806. https://doi.org/10.12988/ijma.2013.13078
[26] Rozaimi Zakaria, Abd F. Wahab, and R. U. Gobithaasan. "Normal Type-2 Fuzzy Interpolating B-Spline Curve." (2014). https://doi.org/10.1063/1.4887635
[27] Rozaimi Zakaria, Abd F. Wahab, Isfarita Ismail, and Mohammad I. E. Zulkifly. "Complex Uncertainty of Surface Data Modeling via the Type-2 Fuzzy B-Spline Model." *Mathematics* 9, no. 9 (2021): 1054. https://doi.org/10.3390/math9091054
[28] Bijan Davvaz, Wiesław A. Dudek, and Y. Jun. "Intuitionistic Fuzzy -Submodules." *Information Sciences* 176, no. 3 (2006): 285–300. https://doi.org/10.1016/j.ins.2004.10.009
[29] Paul Augustine Ejegwal and M. Adamu. "Distances Between Intuitionistic Fuzzy Sets of Second Type With Application to Diagnostic Medicine." *Notes on Intuitionistic Fuzzy Sets* 25, no. 3 (2019): 53–70. https://doi.org/10.7546/nifs.2019.25.3.53-70
[30] Mohammad Izat Emir Zulkifly and Abdul Fatah Wahab. "Visualization of Intuitionistic Fuzzy B-Spline Space Curve and Its Properties." *Educatum Journal of Science Mathematics and Technology* 6, no. 1 (2019): 41–46. https://doi.org/10.37134/ejsmt.vol6.1.6.2019
[31] Abd Fatah Wahab, Mohammad Izat Emir Zulkifly, and Mohd Sallehuddin Husain. "Bezier Curve Modeling for Intuitionistic Fuzzy Data Problem." (2016). https://doi.org/10.1063/1.4954583

[32] Hatice Ercan-Tekşen and Ahmet Sermet Anagün. "Intuitionistic Fuzzy C-Control Charts Using Defuzzification and Likelihood Methods." *Journal of Intelligent & Fuzzy Systems* 39, no. 5 (2020): 6465–6473. https://doi.org/10.3233/jifs-189110
[33] Sanjay Kumar and Sukhdev Singh Gangwar. "A Fuzzy Time Series Forecasting Method Induced by Intuitionistic Fuzzy Sets." *International Journal of Modeling Simulation and Scientific Computing* 06, no. 04 (2015): 1550041. https://doi.org/10.1142/s1793962315500415
[34] Siti Sarah Raseli, Nur Ain Mohd Khusairy Faisal, and Norpah Mahat. "Construction of Cubic Bezier Curve." *Journal of Computing Research and Innovation* 7, no. 2 (2022): 111–120. https://doi.org/10.24191/jcrinn.v7i2.291
[35] Andrea Picardi, Giorgia Ballabio, Venanzio Arquilla, and Giandomenico Caruso. "A Study on Haptic Actuators to Improve the User Experience of Automotive Touchscreen Interfaces." *Computer-Aided Design and Applications* (2024): 136–149. https://doi.org/10.14733/cadaps.2025.136-149
[36] Mabrokah kilani, Almbrok Hussin Alsonosi Omar, Iman Zaky Ahmed, and Fatima Abuzaiyan. "The Quadratic Trigonometric Bezier Like Curve With Two Shape Parameters." *Journal of Pure & Applied Sciences* 22, no. 3 (2023): 215–221. https://doi.org/10.51984/jopas.v22i3.2786
[37] W. M. Mahmoud, M. A. Soliman, and Esraa M. Mohamed. "Investigation on Isotropic Bezier Sweeping Surface "IBSS" With Bishop Frame." *Mathematics and Statistics* 11, no. 2 (2023): 373–378. https://doi.org/10.13189/ms.2023.110216
[38] Jerry M. Mendel, *Uncertain Rule-Based Fuzzy Logic Systems: Introduction and New Directions*. 2001, Upper Saddle River, NJ: Prentice Hall PTR. https://doi.org/10.1007/978-3-319-51370-6
[39] Thomas C. Hanks and Hiroo Kanamori. "A moment magnitude scale." *Journal of Geophysical Research: Solid Earth* 84, no. B5 (1979): 2348–2350. https://doi.org/10.1029/jb084ib05p02348
[40] E. M. Scordilis. "Empirical Global Relations Converting MS and mb to Moment Magnitude." *Journal of Seismology* 10, no. 2 (2006): 225–236. https://doi.org/10.1007/s10950-006-9012-4
[41] Göran Ekström and Adam M. Dziewonski. "Evidence of bias in estimations of earthquake size." *Nature* 332, no. 6162 (1988): 319–323. https://doi.org/10.1038/332319a0
[42] Filiz Tuba Kadirioğlu and Recai Feyiz Kartal. "The New Empirical Magnitude Conversion Relations Using an Improved Earthquake Catalogue for Turkey and Its Near Vicinity (1900–2012)." *Turkish Journal of Earth Sciences* 25 (2016): 300–310. https://doi.org/10.3906/yer-1511-7
[43] D. Stromeyer, Gottfried Grünthal, and Rutger Wahlström. "Chi-Square Regression for Seismic Strength Parameter Relations, and Their Uncertainties, With Applications to an Mw based Earthquake Catalogue for Central, Northern and Northwestern Europe." *Journal of Seismology* 8, no. 1 (2004): 143–153. https://doi.org/10.1023/b:jose.0000009503.80673.51
[44] Hussam Hamrawi, Simon Coupland, and Robert John. "Type-2 Fuzzy Alpha-Cuts." *IEEE Transactions on Fuzzy Systems* 25, no. 3 (2017): 682–692. https://doi.org/10.1109/tfuzz.2016.2574914
[45] Yaya Sudarya Triana and Astari Retnowardhani. "Enhance Interval Width of Crime Forecasting With ARIMA Model-Fuzzy Alpha Cut." *Telkomnika (Telecommunication Computing Electronics and Control)* 17, no. 3 (2019): 1193. https://doi.org/10.12928/telkomnika.v17i3.12233
[46] Siti Nasyitah Jaman, Rozaimi Zakaria, and Isfarita Ismail. "Fuzzy Intuitionistic Alpha-Cut Interpolation Rational Bézier Curve Modeling for Shoreline Island Data." *Malaysian Journal of Fundamental and Applied Sciences* 19, no. 6 (2023): 1142–1151. https://doi.org/10.11113/mjfas.v19n6.3126
[47] Mohammad Ahmad and Weihu Cheng. "A Novel Approach of Fuzzy Control Chart With Fuzzy Process Capability Indices Using Alpha Cut Triangular Fuzzy Number." *Mathematics* 10, no. 19 (2022): 3572. https://doi.org/10.3390/math10193572
[48] K. Arun Prakash, M. Suresh, and S. Vengataasalam. "A New Approach for Ranking of Intuitionistic Fuzzy Numbers Using a Centroid Concept." *Mathematical Sciences* 10, no. 4 (2016): 177–184. https://doi.org/10.1007/s40096-016-0192-y
[49] Dipti Dubey and Aparna Mehra. "Linear Programming With Triangular Intuitionistic Fuzzy Number." (2011). https://doi.org/10.2991/eusflat.2011.78

[50] Feng Feng, Yujuan Zheng, José Carlos R. Alcantud, and Qian Wang. "Minkowski Weighted Score Functions of Intuitionistic Fuzzy Values." *Mathematics* 8, no. 7 (2020): 1143.https://doi.org/10.3390/math8071143

[51] Krassimir T. Atanassov. "Type-1 Fuzzy Sets and Intuitionistic Fuzzy Sets." *Algorithms* 10, no. 3 (2017): 106. https://doi.org/10.3390/a10030106

[52] Eulalia Szmidt and Janusz Kacprzyk. "Distances Between Intuitionistic Fuzzy Sets." *Fuzzy Sets and Systems* 114 (2000): 505–518.https://doi.org/10.1016/s0165-0114(98)00244-9